Emittance Measurements for High Charge State Ion Beams Extracted from the AECR-U Ion Source

D. Wutte*, M. A. Leitner and C. M. Lyneis

Lawrence Berkeley National Laboratory, University of California, 1 Cyclotron Road MS 88, Berkeley, California, 94720, USA

Abstract

In order to investigate the ion-optical parameters of the AECR-U injection line into the 88-Inch Cyclotron, an electrostatic-deflection-type emittance scanner has been designed and constructed. It allows fast on-line measurements, while tuning the ion beam through the cyclotron. Emittance measurements have been performed for various high charge state ions. First results indicate a strong mass dependence of the normalized beam emittance. For example the normalized rms emittance for protons (0.24 π·mm·mrad) is four times higher than for O6+ (0.06 π·mm·mrad) and about 8 times higher than Kr19+ (0.03 π·mm·mrad). Furthermore it was found, that the emittance values are approximately independent of the current at the medium ion beam intensities. The predominant factor on the beam emittance is shown to be the plasma stability. The emittance measurements and the results are discussed in the paper.

1. The AECR-U ion source performance

The AECR-U ion source started operation in 1990, but was substantially upgraded to the current AECR-U in 1996 [1]. The AECR-U ion source is optimized for the production of high charge state ions by combining all of the current ECR ion source improvement techniques, including aluminum chamber walls, two-frequency plasma heating, cold electron injection, radial pumping and strong magnetic confinement. Microwaves of two frequencies, 14 and 10 GHz drive the AECR-U plasma. Six radial slots provide additional pumping of the plasma chamber, which improves the stability and high charge state performance of the ion source. The radial slots also provide easy oven access to the plasma chamber. Up to three different metal ions can be produced with the AECR-U at the same time with two different oven types.

Table I lists some of the high charge state ion beams produced by the AECR-U ion source. The highest charge state accelerated with the 88-Inch Cyclotron was U^{64+}, which is the highest charge state ion extracted so far from an ECR ion source [2].

2. The mass analyzing system and emittance scanner

The mass analyzing beam line section consists of a Glaser lens (magnetic solenoid with iron return yoke), which focuses the beam to the first set of slits at the focal point of the spectrometer magnet. The 90-degree bend magnet analyzes and refocuses the ion beam through a second set of slits on to a Faraday cup (with a secondary electron suppression of -150 V). The 90-degree bending magnet provides a mass resolution of $m/\Delta m = 50$ at the horizontal slit (xx'-plane) opening of 12 mm. The vertical (yy'-plane)

*e-mail: daniela_wutte@lbl.gov, www:http://ecrgroup.lbl.gov

slits are opened to 20 mm. Typical ion beam transmission through the analyzing system at this setting is 50 to 70%. All the emittance measurements were taken at these slit openings.

3. The emittance scanner

The emittance scanner is located 30 cm downstream of the horizontal focal point of the analyzing magnet. The electrostatic-deflection-type emittance scanner has been designed and constructed at the 88-Inch Cyclotron. A detailed description of the mechanical design and the analyzing software can be found elsewhere [3]. The measurement principle [4] is shown in Fig. 1. The beam enters through the entrance slit and gets deflected by parallel plates into a Faraday Cup. The deflection voltage is proportional to the divergence of the beam at this location. As the scanner is moved stepwise through the beam the voltage of the deflection plates is varied at each step to determine the divergence and intensity distribution of the beam at this location.

Table I. *Example high charge state ion beams produced by the LBNL AECR-U (currents measured after the analyzing magnet).*

Ion	I[eμA]	Ion	I[eμA]
Ar^{13+}	120	Ca^{11+}	225
Ne^{6+}	260	Ca^{19+}	0.25
Ne^{9+}	110	Co^{13+}	113
Ar^{17+}	2	V^{12+}	90
Ar^{18}	0.12	Au^{36+}	13
Kr^{19+}	75	Au^{46+}	1
Kr^{28+}	2	Bi^{25+}	85
Xe^{26+}	51	Bi^{50+}	0.15
Xe^{36+}	1	U^{31+}	25
Xe^{38+}	0.25	U^{50+}	0.5
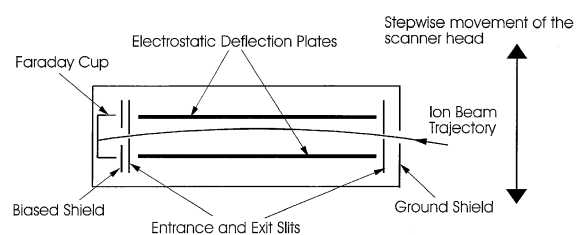
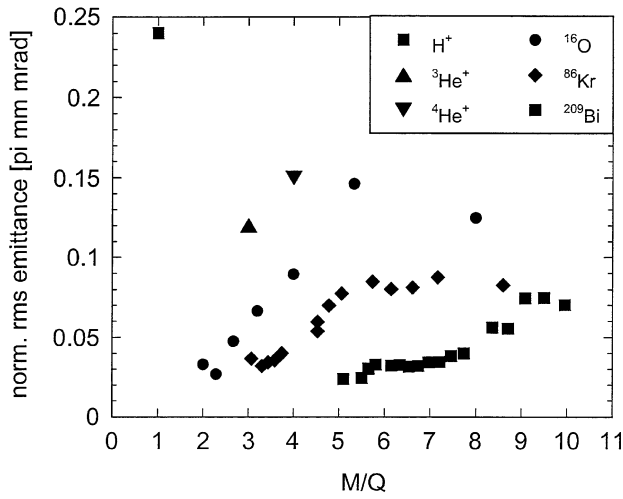*Fig. 1.* Measurement principle of the electrostatic emittance scanner.

Fig. 2. Comparison of the normalized emittance values for different masses and charge states.

The statistical rms emittance is then determined according to

$$\varepsilon_{xrms} = \sqrt{<x^2> \cdot <x'^2> - <x \cdot x'>^2},$$
$$\varepsilon_{yrms} = \sqrt{<y^2> \cdot <y'^2> - <y \cdot y'>^2}, \qquad (1)$$
$$x' = p_x/p_z, \qquad y' = p_y/p_z,$$

with x representing the horizontal axis and y the vertical axis in the plane perpendicular to the beam direction z, and x' and y' representing the angles of divergence. The averages are weighted by the beam intensity.

In order to compare emittances for different masses and charge states, the emittance values are normalized to the longitudinal velocity according to,

$$\varepsilon_{rms,norm} = \varepsilon_{rms} \cdot \beta \cdot \gamma, \qquad \beta = \frac{v}{c}, \quad g = (1 - \beta^2)^{-1/2}. \qquad (2)$$

4. Emittance measurements

Systematic ion beam emittance measurements in both the horizontal (xx') and vertical plane (yy') were performed for a wide range of ions. The dependence of the normalized xx' emittance values for helium and charge state distributions of oxygen, krypton and bismuth on the mass to

charge ratio M/Q is shown in Fig. 2. A similar dependence was measured for the vertical plane. The emittance values for a particular charge state distribution were measured at the same plasma condition, only the settings for the Glaser lens and the analyzing magnet were changed. The emittance decreases systematically with increasing mass, more than can be explained by the concentration of hot electrons on axis. This may be due to cooling of the heavier masses by ion-ion collisions in the plasma.

Within a charge state distribution for a particular element the measured emittance decreases for higher charge states. These results are consistent with the model that highly charged ions are created closer to the center of the ECR plasma, where hot electrons are confined. This hot electron core also confines the highest charge state ions in the electrostatic well. The low charge state ions can be produced at the outer shell of the ECR plasma and therefore have higher emittance values. This is also in agreement with the observation, that the extracted currents for high charge state ions decrease less than those for low charge state ions after reduction of the extraction hole diameter [5].

As an illustration Fig. 3 shows the emittance pattern for O^+ and O^{8+}, $\varepsilon_{norm} = 0.1$ and $\varepsilon_{norm} = 0.03$ π·mm·mrad respectively. O^+ with an ionization potential of 13.6 eV can be created in the outer plasma regions. On the other hand, O^{8+} with an ionization potential of 871 eV is created close to the hot electron region in the source center.

The dependence of the normalized xx' and yy' emittance values on the charge state is shown in detail in Fig. 4 for a bismuth charge state distribution (CSD) optimized for medium charge state ion production. The beam currents measured for each charge are plotted in Fig. 5 for reference.

It is evident, that the emittance value is predominantly dependent on the charge state and not on the current at these ion beam intensities. For instance the ion beam emittance of 18.8 eμA of Bi^{21+} was measured to be 0.07 π·mm·mrad, while the emittance of 18 eμA of Bi^{32+} was 0.03 π·mm·mrad.

Furthermore, the emittance is approximately independent on the current over a wide range of extracted currents for given charge state. For Ar^{9+} the normalized rms emittance values were measured to be 0.067, 0.064, 0.065, 0.058 π·mm·mrad at total extracted currents of 0.75, 0.86, 1.2 and 2 mA, delivering 10, 52, 108 and 145 eμA of Ar^{9+} at 15 kV extraction voltages. The emittance values changed
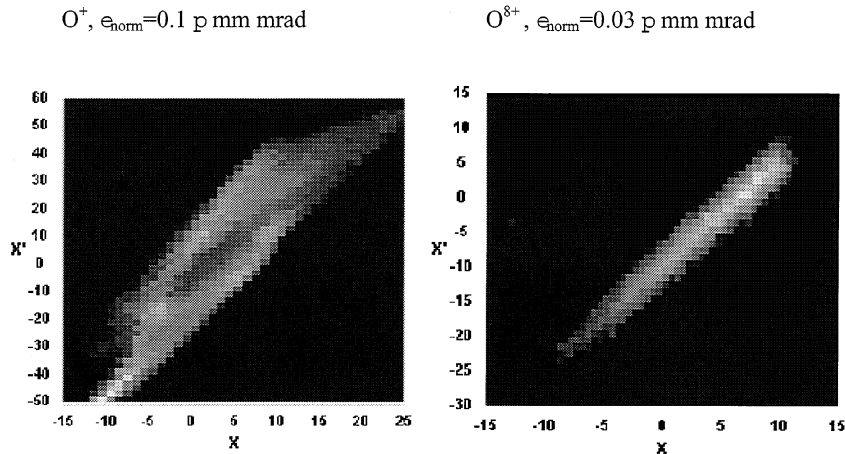
O^+, $e_{norm} = 0.1$ p mm mrad O^{8+}, $e_{norm} = 0.03$ p mm mrad

Fig. 3. Emittance patterns (x' [mrad], x [mm]) for O^+ and O^{8+} (Please note the different axis scales of the two measurements).
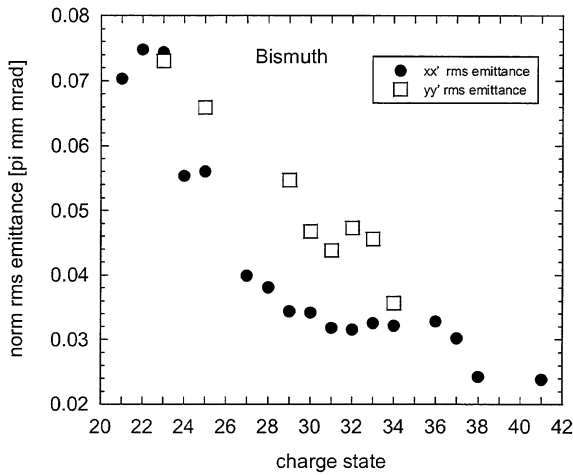
Fig. 4. Dependence of the normalized *xx'* and *yy'* emittance values on the charge state for a bismuth charge state distribution.
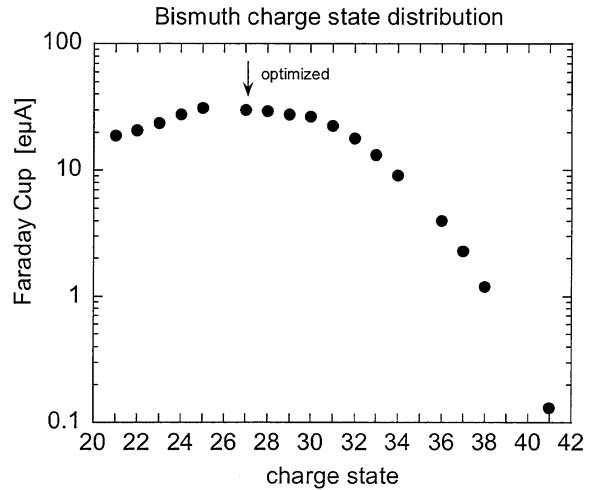

Fig. 5. Bismuth charge state distribution used for the emittance measurements of Fig. 4.
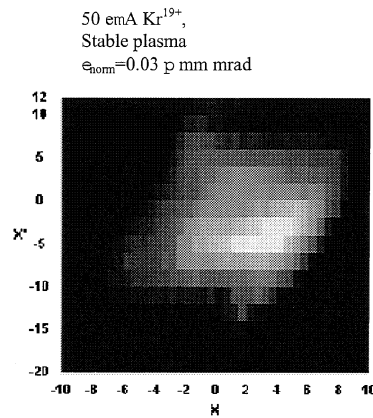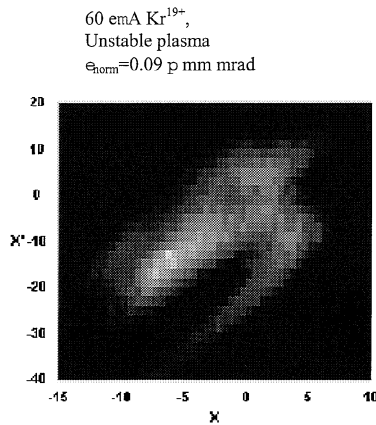

Fig. 6. Emittance patterns (*x'* [mrad], *x* [mm]) of two different ion source tunes for a high intensity $^{86}Kr^{19+}$ beam (Please note the different axis scales of the two measurements).

less than 10% over the mentioned intensity range, the lowest emittance was actually measured at the highest current in this case.

On the other hand for unstable plasma conditions, the ion beam emittance can easily vary a factor of 2 or 3 at comparable ion beam intensity (see Fig. 6). This makes the emittance scanner an extremely useful ion source tuning aid and important step to improve the overall ion beam transmission in the cyclotron injection line. Fig. 6 shows an example of two different ion source tunes for a high intensity $^{86}Kr^{19+}$ beam at comparable currents and rf power levels. The influence of the plasma stability on the ion beam emittance can be clearly seen. The Faraday Cup readings for both tunes are similar, and only the emittance measurement indicates the presence of plasma instabilities.

Acknowledgements

References

1. Xie, Z. Q. and Lyneis, C. M., Proc. 13th International Workshop on ECR Ion Sources, Texas A&M, College Station, USA, 16 (1997).
2. Xie, Z. Q., Lyneis, C. M., Clark, D. J., Guy, A. and Lundgren, S. A., Proc. 15th Conference on Cyclotrons and their Applications 98, Caen, 1998.
3. Leitner, M. A., Wutte, D. and Lyneis, C. M., in prep. To be submitted to Nucl. Instr. Meth. A.
4. Allison, P. W., Sherman, J. D. and Holtkamp, D. B., IEEE Trans. Nucl. Sci. **NS-30**, 2204 (1991).
5. Clark, D. J., Proc. International Conference on ECR Ion Sources, East Lansing, MI, USA, 1987.